

Rapid Communications

Rapid Communications are intended for the accelerated publication of important new results and are therefore given priority treatment both in the editorial office and in production. A Rapid Communication in Physical Review B should be no longer than 4 printed pages and must be accompanied by an abstract. Page proofs are sent to authors.

Surface Fermi contours and phonon anomalies on Pt(111)

Wei Di, Kevin E. Smith, and Stephen D. Kevan

Physics Department, University of Oregon, Eugene, Oregon 97403

(Received 21 January 1991)

The surface Fermi contours of Pt(111) have been determined with use of high-resolution angle-resolved photoemission. There exist two surface resonances which produce distinct Fermi contours. The first contour is an approximately hexagonal electron pocket centered in the surface Brillouin zone and is very nearly degenerate with the edge of the projection of the sixth bulk band. The other contour is a more diffuse triangular electron pocket centered at \bar{K} , and is loosely associated with a projected gap in the fifth bulk band. These results do not support the suggestion that anomalies observed in measurements of the Pt(111) surface-phonon dispersion relations might be caused by screening singularities associated with surface-localized states. Our contours provide a guide for future phonon measurements searching for such anomalies.

With the availability of precise probes for measuring surface-phonon dispersion relations, the possible existence of two-dimensional (2D) phonon anomalies has gained much attention lately.¹⁻⁴ As demonstrated by Kohn,⁵ anomalies (or nonanalyticities) in phonon dispersion relations can arise from near singularities in the generalized electronic susceptibility. These are directly related to the existence of a well-defined Fermi surface, and are located, in the simplest case, at those wave-vector values which are twice the Fermi wave vector. A generalization of this simple idea to systems with complex Fermi surfaces explains the existence of Kohn anomalies in several bulk metals. For example, the group-VIII metals platinum and palladium exhibit pronounced kinks in the phonon dispersions along the $\bar{\Sigma}$ line of the bulk Brillouin zone which are associated with transitions across the "jungle-gym" portion of the Fermi surface formed by the fifth bulk band.^{6,7} Such observations provide important information on nonadiabatic electron-phonon coupling dynamics in metals. In addition, the existence of these anomalies provides one mechanism whereby a lattice might reconstruct to form a larger, possibly incommensurate unit cell.^{4,8,9} Such phenomena are at the heart of issues concerning a material's stability, and are thus of particular interest within the surface physics community since surface lattices often reconstruct.

The lowered dimensionality of intrinsic surface electron states favors production of screening singularities and phonon anomalies, and thus possibly of surface reconstruction.^{4,8,9} The existence of phonon anomalies on Pt(111) produced by coupling to intrinsically 2D surface states has been the subject of significant controversy recently. Two groups, using inelastic helium scattering spectroscopy, have proposed the existence of two anomalies in the surface-phonon dispersion relations along the

$[\bar{1}\bar{1}0]$ direction at momenta of 0.8 and 1.2 \AA^{-1} .^{1,2} It was suggested that at least one of these was caused by Fermi contours of surface-localized states.¹ However, a third experiment did not observe these anomalies.³ Moreover, a theoretical calculation carried out by Bortolani *et al.*,¹⁰ suggested that one of the proposed anomalies might be mistaken, and that the other one might merely be a projection of the well-known bulk anomaly onto the surface. An accurately measured 2D Fermi surface of the surface-localized electronic states in Pt(111) surface should provide some clarification of these issues. In this paper, we report such a measurement using high-resolution angular-resolved photoemission (ARP) spectroscopy. In support of Bortolani's calculation, our results give no evidence that either of the reported anomalies is associated with surface-localized Fermi contours. On the other hand, we do observe large-scale nesting at a well-defined wave-vector larger in magnitude than measured in the surface-phonon experiments. This result suggests further phonon measurements on this surface might be in order.

Our ARP system, located at the National Synchrotron Light Source at Brookhaven National Laboratory, has been described in detail previously.^{11,12} The total instrumental energy and angular resolutions are typically less than 120 meV and 1°, respectively, at full width at half maximum. A 99.999%-purity Pt(111) crystal 1 cm diam \times 0.5 mm thick was oriented to within 0.5° of the [111] bulk crystalline axis by Laue x-ray backreflection. The surface was first prepared by mechanical polishing and chemical etching in hot aqua regia, and then inserted into our vacuum system. After many cycles of heating to 1000 K in oxygen, or occasionally neon ion sputtering at 700 K, followed by annealing at 1200 K, an extremely clean and well-ordered surface was prepared as determined by low-energy electron diffraction and Auger elec-

tron spectroscopy. The surface remained clean for typically 30–45 min at an operating pressure of $(0.8\text{--}1.2)\times 10^{-10}$ Torr, as evidenced by the gradual disappearance of some of the more contamination-sensitive features in the photoemission spectrum. The residual surface contaminants (CO and H) were thermally desorbed by flashing the crystal to 800–1200 K every 20–30 min.

The basic procedure for measuring the Fermi surface of the surface-localized states has been used in several of our previous studies.^{13–15} We simply extrapolate measured surface-state (or resonance) dispersion curves to the Fermi level to determine one point on the 2D Fermi contour. For example, in Fig. 1 we present a series of the photoemission spectra for clean and hydrogen covered Pt(111). These were taken along the \bar{T} line ($\bar{\Gamma}\text{--}\bar{K}$ or $[1\bar{1}0]$ direction) of the surface Brillouin zone (SBZ). The displayed spectra were collected at photon energy of 24 eV over a range of momenta parallel to the surface of $0.64\text{ \AA}^{-1} \leq k_{\parallel} \leq 1.50\text{ \AA}^{-1}$. The two peaks indicated by the dashed guidelines are observed to be quenched or substantially reduced by hydrogen adsorption. They are not true surface states, however, as both of these lie within the continuum of the projection of Pt bulk bands onto the SBZ. They are, therefore, accurately labeled surface resonances; this point is discussed further below. The momenta at which these peaks cross the Fermi level, $k_{\parallel}=0.83\text{ \AA}^{-1}$ and $k_{\parallel}=1.20\text{ \AA}^{-1}$, produce two points of the 2D Fermi sur-

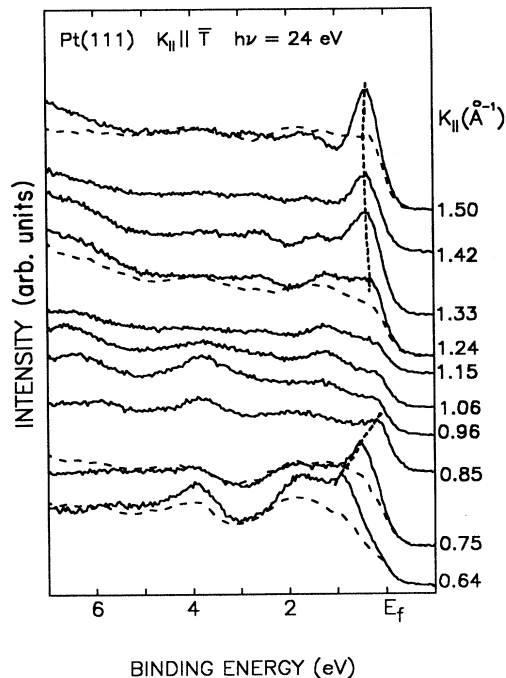


FIG. 1. ARP spectra of Pt(111) at a photon energy of 24 eV, collected with even polarization as a function of electron emission angle in the \bar{T} mirror symmetry plane. The spectra are labeled by the parallel momentum of electrons photoemitted from the Fermi level. The dashed spectra shown for comparison at a few momenta were collected from the hydrogen-saturated surface.

face of Pt(111) in the $(1\bar{1}0)$ mirror symmetry plane. Applying the same procedure to other directions allows us to determine other crossing points, and thereby to map out the complete 2D Fermi contours throughout the SBZ. The number of such crossings we need to produce a complete Fermi contour is much reduced by taking advantage of the rotational symmetry for this surface.

We acknowledge some ambiguity in determining the precise wave vector at which a particular feature crosses E_F . However, the uncertainty is systematic so that the shapes of the contours are accurate although the sizes might be in error by as much as 0.02 \AA^{-1} . Our accuracy in determining the Fermi wave vector (\mathbf{k}_F) compares favorably with that attained by assigning \mathbf{k}_F to the momentum at which the ARP intensity at E_F maximizes.¹⁶ The latter procedure is more time consuming with our apparatus, but, in principle, leads to smaller systematic errors. The systematic error in our procedure was found to be comparable to the random errors evident in our measured contours.

Our results are summarized in Fig. 2, which shows the 2D Fermi contours of clean Pt(111) associated with the

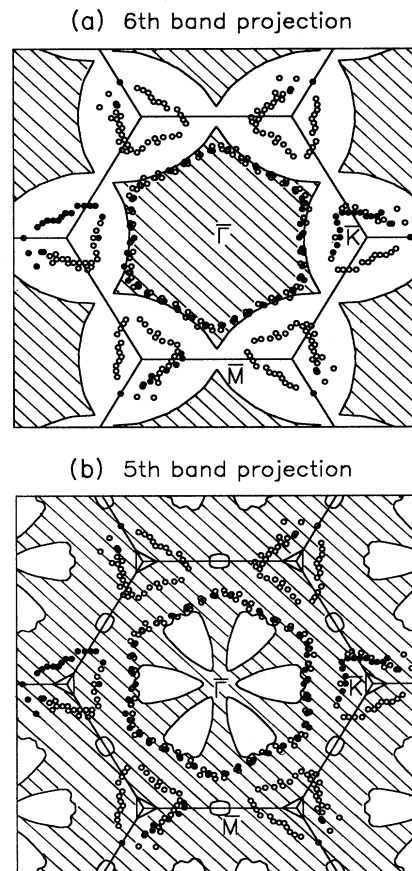


FIG. 2. Experimental surface Fermi contours. Solid circles are measured points, while open circles have been produced by forcing the sixfold rotational symmetry expected for true surface states. Shaded regions correspond to calculated projections of the Fermi surfaces formed by bulk bands (a) 6 and (b) 5.

two resonances discussed above. The shaded regions correspond to the projection onto the (111) SBZ of the bulk Fermi surfaces formed by (a) band 6 and (b) band 5. These projections were calculated using a nonorthogonal tight-binding interpolation scheme,¹⁷ and checked at selected points against the bulk Fermi surface.^{7,18} In the surface contours, two electron pockets exist. One is centered at $\bar{\Gamma}$, and is shaped roughly like a hexagon. This contour is associated with the peak which crosses E_F closer to the zone center in Fig. 1. The other contour, located around each corner point \bar{K} of the surface Brillouin zone, is shaped roughly like an equilateral triangle.

It is interesting to notice that the hexagonal pocket is nearly degenerate with the edge of the projection of the sixth bulk band [Fig. 2(a)]. This behavior has been qualitatively observed on tungsten and molybdenum surfaces,^{13–15} although in those cases the surface bands are often true states. Like the sixth bulk band, the surface band which forms the hexagonal pocket is observed to have a fairly large and nearly isotropic Fermi velocity of $v_F \sim 3 \text{ eV/\AA}^{-1}$. The measured Fermi wave vector does not depend on photon energy and thus on the normal momentum k_{\perp} . The Fermi contour exhibits sixfold symmetry, as would be the case for a true state. In these ways, the band which forms this contour behaves very much like a true surface state. One can think of it as being a resonant enhancement of the sixth bulk band edge near the surface plane. If the surface perturbation were more severe, a true state would presumably split from the continuum formed by the sixth bulk band. Given the apparent surface localization, this contour could significantly impact the electronic susceptibility near the surface.

The triangular pocket near \bar{K} exhibits markedly different behaviors from the first pocket. Like the fifth bulk band, the surface band which gives rise to the triangular pocket has a fairly small Fermi velocity ($\sim 1 \text{ eV/\AA}^{-1}$). The associated ARP feature is never clearly resolved from E_F , attaining a maximum binding energy at \bar{K} of about 0.25 eV. Moreover, the Fermi wave vector depends upon k_{\perp} , and the pockets on opposite sides of the normal do not exactly mirror one another, implying a deviation from true sixfold symmetry. The triangular contours reproduced in Fig. 2 were forced to have sixfold symmetry and should thus be taken to be indistinct. While much of the resonant weight crosses E_F as indicated, the band actually brackets E_F over the entire triangular pocket and even somewhat beyond. This pocket is resonant with continuum formed by the fifth bulk band [Fig. 2(b)], surrounding a small projected triangular gap at \bar{K} . While the pocket also fits nicely into the pseudo-triangular-shaped gaps in the sixth bulk band projection [Fig. 2(a)], its behaviors indicate that it is more closely associated with bulk states in the fifth band.

Ignoring matrix element effects, the momenta where the surface-phonon anomalies might occur on Pt(111) can be predicted by the nesting of contours in the 2D Fermi surface in Fig. 2. For example, the opposite sides of the hexagonal contour are nearly flat and are necessarily parallel to each other. Thus the joint density of states for creating electron-hole pairs with a momentum exactly

spanning the two sides would be fairly large. In this way, we can predict that a Kohn anomaly might exist at the nested momentum vector of $2\mathbf{k}_F = 1.70 \text{ \AA}^{-1}$ or $G_{[1\bar{1}0]} - 2\mathbf{k}_F = 2.83 \text{ \AA}^{-1}$ in the $[1\bar{1}0]$ direction. The precise momenta of the anomalies might be shifted slightly if the electron-phonon coupling matrix elements are substantially momentum dependent.¹⁹ The hexagonal contour is less efficiently nested along the $\bar{\Sigma}$ line; we thus predict a much smaller anomaly would be observed in that azimuth. Unfortunately, all the surface-phonon measurements were terminated at momenta near the \bar{K} point, $k_{\parallel} = 1.5 \text{ \AA}^{-1}$. The anomaly predicted here, if it exists, was not measured for this reason. We suggest that the phonon measurements be extended to the second SBZ zone in the $[1\bar{1}0]$ direction, with special attention paid to the vicinity of $k_{\parallel} = 1.7 \text{ \AA}^{-1}$.

In the same direction, Kohn anomalies due to couplings involving the triangular contours might also be predicted. However, the indistinct nature of this contour implies that the anomalies would be spread over a fairly broad range of momenta. For example, if we recall that the band brackets E_F inside the entire pocket, we see that phonon wave vectors between 0.8 and 2.0 \AA^{-1} along the \bar{T} line might be affected. Stated another way, one thinks of a Kohn anomaly as being localized in momentum space, whereas couplings involving this contour would be somewhat delocalized. Its impact might be manifested by minor changes in force constants in the surface region, thereby impacting the surface-phonon branches over a large fraction of the SBZ.

The phonon measurements suggested that anomalies occur at $k_{\parallel} = 0.8$ and 1.2 \AA^{-1} in the \bar{T} azimuthal direction. The wave vector of our predicted anomaly arising from the hexagonal contour is significantly larger than either of these. It is unlikely that momentum-dependent electron-phonon coupling matrix elements could account for this large difference. Both suggested anomalies lie within the range of momenta which might be affected by the triangular contour. However, our results do not suggest anything special about these two momenta. Consider, for example, the flat faces of the triangular pocket. Even though these are resonantly broadened by coupling to bulk states, the “centroids” appear to be well-nested and thus might lead to an anomaly. However, the coupling momentum between these two is roughly 2.0 \AA^{-1} and is thus much larger than either suggested anomaly. We thus see that our surface Fermi contours do not support an origin involving surface-localized states. This observation is generally in accord with the work of Bortolani *et al.*¹⁰

Finally, it is interesting to consider the stability of the Pt(111) surface with respect to the Fermi contours in Fig. 2. One might expect this surface to undergo a Peierls-like, charge-density-wave reconstruction with a wave vector determined by the flat faces of the hexagonal pocket. Qualitatively, this orbit is strikingly similar to that calculated for a variety of quasi-2D transition metal compounds which are observed to reconstruct.²⁰ That Pt(111) has not been observed to reconstruct at any temperature is an interesting negative result. The propensity to undergo a Peierls-like reconstruction is determined by a competi-

tion between decreasing kinetic energy from production of charge-density-wave gaps and increasing lattice strain energy associated with the periodic distortion, and by the magnitude of the electron-phonon coupling matrix elements. The kinetic-energy decrease is determined in part by the joint density of states at the nesting wave vector. This is enhanced by the small curvature of the hexagonal contour near the $\bar{\Gamma}$ line, but decreased by the fairly large Fermi velocity and by any resonant broadening of the surface band. The strain energy induced by any reconstruction would be fairly large, because the surface is a close-packed hexagonal lattice and because the underlying layers would presumably retain the undistorted structure.

Apparently, this strain dominates and an unreconstructed surface results.

We would like to thank Kuang Jen Wu for preparing and cleaning the sample. This work was carried out in part at the National Synchrotron Light Source at Brookhaven National Laboratory which is supported by the U.S. Department of Energy, Division of Materials Science and Division of Chemical Sciences. Financial support from the U.S. Department of Energy under Grant No. DE-FG06-86ER45275 is gratefully acknowledged. The work of S.D.K. was supported by the National Science Foundation and the Alfred P. Sloan Foundation.

-
- ¹U. Harten, J. P. Toennies, C. Woll, and G. Zhang, *Phys. Rev. Lett.* **55**, 2308 (1985).
- ²D. Neuhaus, F. Joo, and B. Feuerbacher, *Surf. Sci.* **165**, L90 (1986).
- ³K. Kern, R. David, R. L. Palmer, G. Comsa, and T. S. Rahman, *Phys. Rev. B* **33**, 4334 (1986); *Surf. Sci.* **178**, 537 (1986).
- ⁴H. H. Ernst, E. Hulpke, and J. P. Toennies, *Phys. Rev. Lett.* **58**, 1941 (1987).
- ⁵W. Kohn, *Phys. Rev. Lett.* **2**, 393 (1959).
- ⁶A. P. Miller and B. N. Brockhouse, *Can. J. Phys.* **49**, 704 (1971); D. H. Dutton, B. N. Brockhouse, and A. P. Miller, *Can. J. Phys.* **50**, 2915 (1972).
- ⁷O. K. Andersen, *Phys. Rev. B* **2**, 883 (1970).
- ⁸E. Tosatti, *Solid State Commun.* **25**, 637 (1978).
- ⁹A. J. Freeman, T. J. Watson-Yang, and J. Rath, *J. Magn. Mater.* **12**, 140 (1979).
- ¹⁰V. Bortolani, A. Franchini, G. Santoro, J. P. Toennies, Ch. Woll, and G. Zhang, *Phys. Rev. B* **40**, 3524 (1989).
- ¹¹S. D. Kevan, *Rev. Sci. Instrum.* **54**, 1441 (1983).
- ¹²P. Thiry, P. A. Bennett, S. D. Kevan, W. A. Royer, E. E. Chaban, J. E. Rowe, and N. V. Smith, *Nucl. Instrum. Methods Phys. Rev. Sect. B* **222**, 85 (1984).
- ¹³R. H. Gaylord, K. Jeong, and S. D. Kevan, *Phys. Rev. Lett.* **62**, 2036 (1989).
- ¹⁴K. Jeong, R. H. Gaylord, and S. D. Kevan, *Phys. Rev. B* **39**, 2973 (1989).
- ¹⁵K. E. Smith, G. S. Elliott, and S. D. Kevan, *Phys. Rev. B* **42**, 5385 (1990).
- ¹⁶S. Dhar and S. D. Kevan, *Phys. Rev. B* **41**, 8516 (1990).
- ¹⁷D. A. Papaconstantopoulos, *Handbook of the Band Structure of Elemental Solids* (Plenum, New York, 1986).
- ¹⁸J. B. Ketterson and L. R. Windmiller, *Phys. Rev. Lett.* **20**, 321 (1968); L. R. Windmiller and J. B. Ketterson, *ibid.* **20**, 324 (1968); J. B. Ketterson, M. Mueller, and L. R. Windmiller, *Phys. Rev.* **186**, 656 (1969).
- ¹⁹X. W. Wang and W. Weber, *Phys. Rev. Lett.* **58**, 1452 (1987); X. W. Wang, C. T. Chan, K. M. Ho, and W. Weber, *ibid.* **60**, 2066 (1988).
- ²⁰J. A. Wilson, F. J. Di Salvo, and S. Mahajan, *Adv. Phys.* **24**, 117 (1975).